Pergamon

0094-114X(95)00006-2

Mech. Mach. Theory Vol. 30, No. 6, pp. 777–789, 1995

0094-114X/95 $9.50 + 0.00

A MATHEMATICAL MODEL OF THE ZE-TYPE WORM GEAR SET

CHUNG-BIAU TSAY,† JIUN-WEN JENG and HONG-SHENG FENG

Department of Mechanical Engineering, National Chiao Tung University, Hsinchu, Taiwan 30050, Republic of China

(Received 26 June 1994; received for publication 31 January 1995)

Abstract—The mathematical model of the ZE-type worm gear set derived here is based on tool design parameters, machine tool settings, and worm and worm-gear cutting mechanisms. The backlash of the worm gear set is considered into the developed mathematical model. The developed mathematical model is most helpful in designing, contact and stress analyzing, manufacturing, measuring and optimizing worm gear sets. The profile of the fly cutter for small-lot worm-gear cutting is also investigated. Three-dimensional computer graphs of the worm gear set are presented to demonstrate the developed mathematical model.

INTRODUCTION

The worm gear set is a primary transmission device used by industry to transmit torque between crossed axes. Due to their high transmission ratios, which can be set from 4 to 400, compact structure and low noise, worm gear sets are widely used in gear-reduction mechanisms.

Previous researchers have made significant contributions to the manufacturing of worm tooth surfaces. Bosch [1], Simon [2], and Oiwa *et al.* [3] proposed different methods of obtaining a more precise worm gear set. Pencil-type milling cutters and disk-type grinding wheels for generation of worm surfaces were studied by Litvin [4]. Winter *et al.* [5] proposed a calculation method for different tooth profiles of cylindrical worms. Worm tooth surfaces manufactured by a generating surface formed by the relative motion of an initial curve (a dresser's curve) were investigated by Zheng *et al.* [6, 7]. Contact surface topology of worm-gear teeth was studied by Janninck *et al.* [8]. Litvin *et al.* [9] studied the limitations of conjugate gear tooth surfaces. Concurrently, limitation of worm and worm-gear surfaces to avoid undercutting was investigated by Kin [10], and Tsai *et al.* [11] studied torque parameters and mathematical models of worm gear sets. Computer-aided design geometric modeling of worms and their machining tools was developed by Bär [12]. A mathematical model for applying the over-wire measurement to worm-thread surface measurement was investigated by Cheng *et al.* [13]. Litvin *et al.* [14] performed computerized simulation of meshing and bearing contact for single-enveloping worm-gear drives. Meanwhile, Simon [15] studied the characteristics of double-enveloping worm-gear drives.

Based on geometry and DIN standards, worm gear sets can be categorized into four main types: ZA, ZN, ZE (or ZI) and ZK. This paper concerns the ZE-type worm gear set. The section of the ZE-type worm perpendicular to the axis of worm rotation is an involute shape. Up to now, two types of mathematical model have been developed for the ZE-type worm gear set. The mathematical model proposed by Litvin *et al.* [3], which is based on the concept of generation line, was the simplest form or equation for the ZE-type worm gear set, and made it easy to simulate the contact process of the worm gear set. The mathematical model of the ZE-type worm proposed by Cheng *et al.* [14] was based on the concept of geometry transformation. The equations developed for the worm are easy to model the over-wire measurement process.

In this paper, a mathematical model for the ZE-type worm gear set is developed based on tool design parameters and machine tool settings. The worm is cut by the screw motion of two cutters with straight-edged profiles, and the worm gear is produced by a hob cutter identical to the worm profile. Using this model, it is easy to modify the worm's surfaces simply by changing the tool design parameters or the machine tool settings. However, the oversize worm-type hob cutter is

†To whom all correspondence should be addressed.

widely used in industry for worm-gear production. In this case, the worm-gear tooth profiles can be obtained by modifying the configuration and machine tool settings of the oversize worm-type hob cutter. The contact of the above-mentioned worm gear set becomes a point contact instead of a line contact. Due to the deformation of the gear tooth surface, the contact point of the worm gear set is spread over an elliptical area under load. The bearing contact of the worm gear set is a set of contact ellipses. Therefore, by modifying design parameters of the oversize worm-type hob cutter, such as its pitch diameter, and machine tool settings, we can extend our research to the worm gear set produced by an oversize worm-type hob cutter.

In this research, the profile of the fly cutter for small-lot worm-gear cutting, and worm-gear backlash are also investigated. Based on the mathematical model of the worm gear set, the precise coordinates of any point on the tooth surfaces of a worm gear set can be calculated. The calculated precise coordinates of the tooth surfaces of worm gear set can be considered as the standard, and used to check the measured data of the product. Computer graphics of the ZE-type worm gear set are presented to demonstrate the developed mathematical model. In addition, the developed mathematical model enables us to simulate the tooth contact analysis (TCA) of the worm gear set. It can also be applied to the finite element gear stress analysis, kinematic error analysis, bearing contact, as well as the optimization of tooth profile and contact pattern of the worm gear set. Therefore, the developed mathematical model is most helpful in designing, analyzing and manufacturing worm gear sets.

DESIGN CONCEPT OF THE ZE-TYPE WORM GEAR SET

One of the characteristics of the ZE-type worm is that its projection on the cross-section perpendicular to the rotation axis is an involute curve, as shown in Fig. 1. For comparison, three different axial cross-section of ZE-type worms are also shown in Fig. 1. Cross-sections B and C are on planes tangent to the base cylinder. The profiles of the ZE-type worms in cross-sections B and C are straight lines on one side, and convex shapes on the other side. Therefore, the ZE-type worm profile can be generated by the screw motion of two cutters with straight-edged profiles. However, these two straight-edged cutters should be placed on planes parallel to each other and tangent to the base cylinder. Based on this concept, a mathematical model of the worm profile can be developed.

The worm-gear can be designed to be generated by a worm-type hob cutter, and the generation mechanism is similar to the meshing mechanism of a worm gear set. The worm-type hob cutter

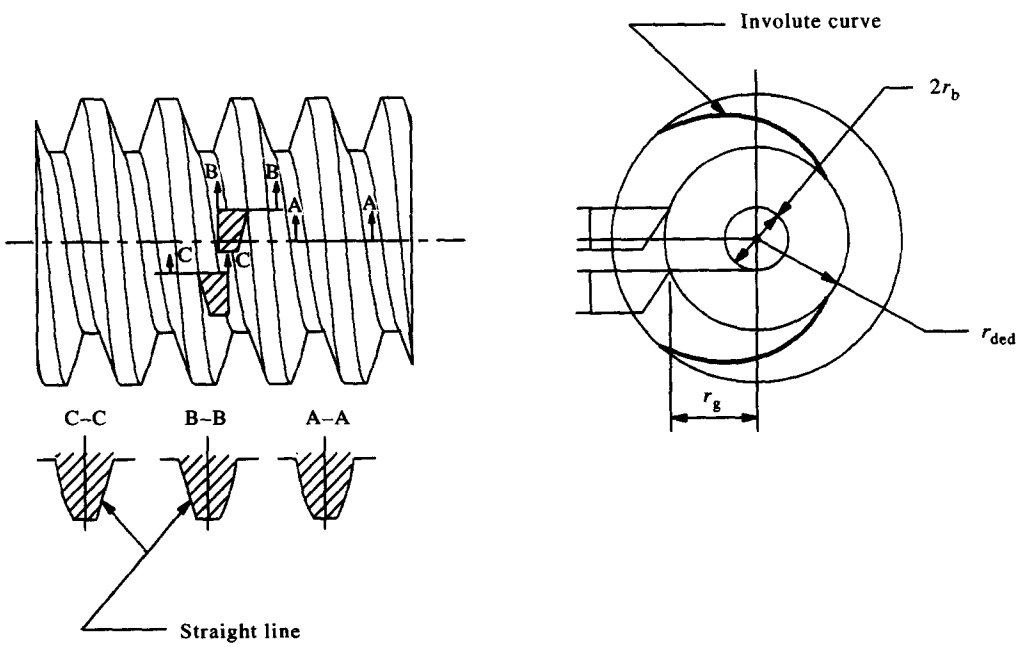

Fig. 1. Cross-section and profile of the ZE-type worm.

and the worm-gear form a conjugate kinematic pair during their generation process. This means that the equation of meshing must be developed first, then the mathematical model of the worm-gear can be obtained by finding the locus envelope of the worm-type hob cutter which is represented in the worm-gear coordinate system. The developed mathematical model of the worm and worm-gear provides precise surface coordinates of any point on worm and worm-gear surfaces.

MATHEMATICAL MODEL OF WORM SURFACE CUTTERS

ZE-type worms can be produced on a lathe using two cutters with straight-edged profiles. These cutters should be set parallel to each other on planes tangent to the worm's base cylinder, as shown in Fig. 1.

The cutter coordinate systems for producing ZE-type worms are represented in Fig. 2. Coordinate system $S_r(X_r, Y_r, Z_r)$ is associated with the right-side cutter, and $S_l(X_l, Y_l, Z_l)$ is associated with the left-side cutter. The design parameters of the cutter are u and α. Parameter u represents the cutter surface coordinate along the straight edge, and α is the tip angle of the cutter. Parameter r_g is the tool offset and is determined by the radii of base cylinder r_b and dedendum cylinder r_{ded} of the worm, as shown in Figs 1 and 2. Based on the geometry shown in Fig. 2, the mathematical model of the straight-edged cutter can be obtained as follows:

(1) for the right-side cutter

$$x_r = -(u \cos\alpha + r_g),$$

$$y_r = 0$$

and

$$z_r = u \sin\alpha. \tag{1}$$

(2) for the left-side cutter

$$x_l = -(u \cos\alpha + r_g),$$

$$y_l = 0$$

and

$$z_l = -u \sin\alpha. \tag{2}$$

MATHEMATICAL MODEL OF THE WORM SURFACE

The ZE-type worm surface, a screw surface which can be generated by a straight-line, performs a screw motion. The right-side and left-side cutters generate the left-side and right-side worm surfaces, respectively. Figure 3 shows the relation between worm and cutter coordinate systems. Coordinate systems $S_r(X_r, Y_r, Z_r)$, $S_l(X_l, Y_l, Z_l)$ and $S_2(X_2, Y_2, Z_2)$ are associated with the

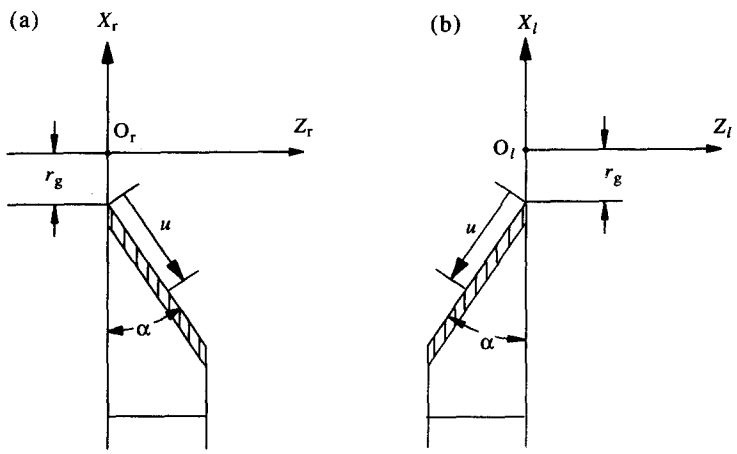

Fig. 2. (a) Right-side cutter, (b) left-side cutter.

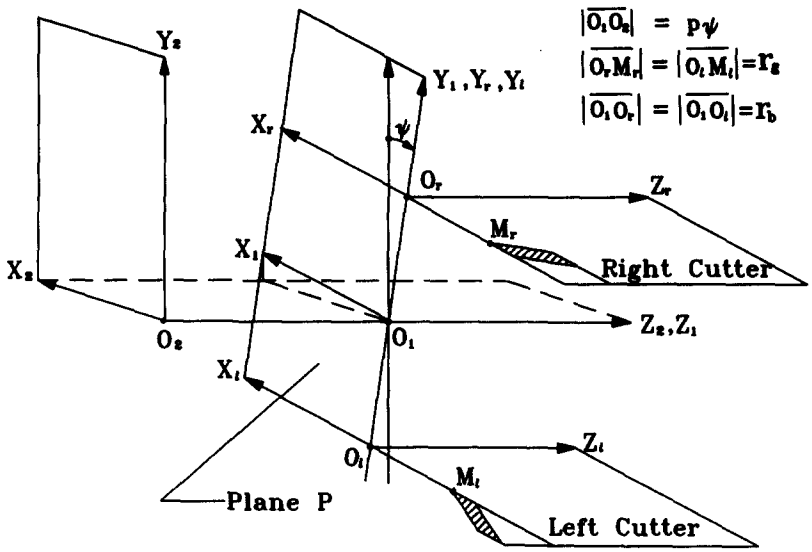

Fig. 3. Relationship between the worm and cutter coordinate systems.

right-side cutter, left-side cutter and worm surface, respectively. Coordinate system $S_1(X_1, Y_1, Z_1)$ is the reference coordinate system; coordinate systems S_r and S_t are rigidly connected to coordinate system S_1 which describes a screw motion with respect to coordinate system S_2; axis Z_2 is the axis of the screw motion.

The left-side worm surface can be considered the locus of the right-side cutter represented in coordinate system $S_2(X_2, Y_2, Z_2)$. Therefore, the equation of the left-side worm surface can be obtained by applying the following homogeneous coordinates transformation matrix equation:

$$\mathbf{R}_2^l = [M_{21}][M_{1r}]\mathbf{R}_r \tag{3}$$

where

$$[M_{1r}] = \begin{bmatrix} 1 & 0 & 0 & 0 \\ 0 & 1 & 0 & r_b \\ 0 & 0 & 1 & 0 \\ 0 & 0 & 0 & 1 \end{bmatrix},$$

$$[M_{21}] = \begin{bmatrix} \cos\psi & -\sin\psi & 0 & 0 \\ \sin\psi & \cos\psi & 0 & 0 \\ 0 & 0 & 1 & p\psi \\ 0 & 0 & 0 & 1 \end{bmatrix}$$

and vector column $\mathbf{R}_r$ is the position vector of the right-side cutter represented in equation (1), and $\mathbf{R}_2^l$ is the position vector of the left-side worm surface represented in coordinate system S_2. The homogenous coordinate transformation matrix $[M_{ij}]$ ($i = 2, 1$ and $j = 1, r$) transforms the position vector from coordinate system S_j to coordinate system S_i. Parameter p is the lead of the worm surface per radian revolution, and ψ is the screw motion surface rotation angle of the cutter with respect to the worm in units of radian. By substituting equation (1) into equation (3), the left-side worm surface is obtained as follows:

$$\mathbf{R}_2^l = \begin{bmatrix} -u\cos\alpha + r_g)\cos\psi - r_b\sin\psi \\ -(u\cos\alpha + r_g)\sin\psi + r_b\cos\psi \\ u\sin\alpha + p\psi \end{bmatrix}. \tag{4}$$

Similarly, the same homogenous coordinate transformation matrix equation can also be used to obtain the right-side worm surface. Nevertheless, position vector $\mathbf{R}_r$ should be replaced by $\mathbf{R}_l$, and the transformation matrix $[M_{1r}]$ is substituted by $[M_{1l}]$ as follows:

$$[M_{1l}] = \begin{bmatrix} 1 & 0 & 0 & 0 \\ 0 & 1 & 0 & -r_b \\ 0 & 0 & 1 & 0 \\ 0 & 0 & 0 & 1 \end{bmatrix}. \tag{5}$$

By substituting equations (2) and (5) into equation (3), the mathematical model of the right-side worm surface can also be obtained as follows:

$$\mathbf{R}_2^l = \begin{bmatrix} -(u\cos\alpha + r_g)\cos\psi + r_b\sin\psi \\ -(u\cos\alpha + r_g)\sin\psi - r_b\cos\psi \\ -u\sin\alpha + p\psi \end{bmatrix}. \tag{6}$$

WORM SURFACE MODIFICATION

The tip point M_r of the right-side cutter and the tip point M_l of the left-side cutter are located in the same plane P which is perpendicular to Z_2 as shown in Fig. 3. In general, the axial tooth thickness and space width of the generated worm surface are not the same. Therefore, the worm surfaces expressed in equations (4) and (6) should be modified. The steps for the modification are listed below.

1. Find the value of cutter parameter u, corresponding to the pitch cylinder, represented in the straight-edged cutter coordinate system.
2. Based on the calculated value of u and the constraint of $X_2 = 0$, the axial difference between the right-side and the left-side worm surfaces on the pitch cylinder can be obtained. Let the amount of this axial difference be denoted by Δz.
3. Comparing the value Δz with the theoretical axial tooth thickness $\pi m/2$, let us define $2S_0 = |\pi m/2 - \Delta z|$.
4. For symmetry, $2S_0$ is equally divided into two parts as the modified amount for the right-side and left-side worm surfaces modification.
5. Add the calculated modified amount S_0 to the Z_2 components of equations (4) and (6) to get the proper worm surface equations. This makes the right-side and left-side cutters symmetric along the Z_2 axis on the plane $Z_2 = 0$.

After considering the steps listed above together with the developed worm surface equations, the modified left-side worm surface equation is obtained as follows:

$$x_2^l = -(u\cos\alpha + r_g)\cos\psi - r_b\sin\psi,$$

$$y_2^l = -(u\cos\alpha + r_g)\sin\psi + r_b\cos\psi$$

and

$$z_2^l = u\sin\alpha + p\psi + S_0. \tag{7}$$

Similarly, the right-side worm surface equation is obtained as follows:

$$x_2^r = -(u\cos\alpha + r_g)\cos\psi + r_b\sin\psi,$$

$$y_2^r = -(u\cos\alpha + r_g)\sin\psi - r_b\cos\psi$$

and

$$z_2^r = -u\sin\alpha + p\psi - S_0. \tag{8}$$

Based on the geometric relationship between the addendum circle and dedendum circle, it is known that any point on the worm surface is located between the radii of dedendum circle r_{ded} and addendum circle r_{add}. This yields

$$r_{ded} \leqslant \sqrt{x_2^2 + y_2^2} \leqslant r_{add}. \tag{9}$$

According to equation (9), the two limiting values of cutter parameter u can be determined.

Some important design parameters of the worm gear set are given by (1) gear set: module = 8.00 mm, (2) worm: number of thread = 1, pitch dia = 80.00 mm, base cyclinder dia = 21.10 mm, addendum cyclinder dia = 96.00 mm and dedendum cylinder dia = 60.97 mm, (3) worm-gear: number of teeth = 30, pitch dia = 240.00 mm, addendum cylinder dia = 255.84 mm and dedendum cylinder dia = 220.82 mm. Based on the calculated limiting values of u and equations (7) and (8), a three-dimensional computer graph of the left-side and right-side worm surfaces can be obtained as shown in Fig. 4.

WORM-GEAR PRODUCTION CONCEPTS

Because worm-gears mate with worms, they can be cut with a worm-type hob cutter, and the cutting process is similar to the mating action of the worm gear set. This cutting/mating mechanism is shown in Fig. 5. The coordinate system, $S_2(X_2, Y_2, Z_2)$ is associated with the worm, the coordinate system $S_3(X_3, Y_3, Z_3)$ is associated with the worm-gear, and the fixed coordinate systems $S_A(X_A, Y_A, Z_A)$, $S_B(X_B, Y_B, Z_B)$ and $S_C(X_C, Y_C, Z_C)$ are the reference systems. In the worm-gear cutting process, the worm is replaced by a worm-type hob cutter which cuts worm-gear. In the cutting simulation, the worm-type hob cutter rotates about axis Z_A through an angle ψ_1 with respect to the reference coordinate system S_A while the worm-gear rotates about Z_C axis through an angle ψ_2 with respect to the reference coordinate system S_C. In order to develop the mathematical model of the worm-gear, it is necessary to find the locus equation of the worm-type hob cutter, and the equation of meshing of the worm-type hob cutter and the worm-gear. For

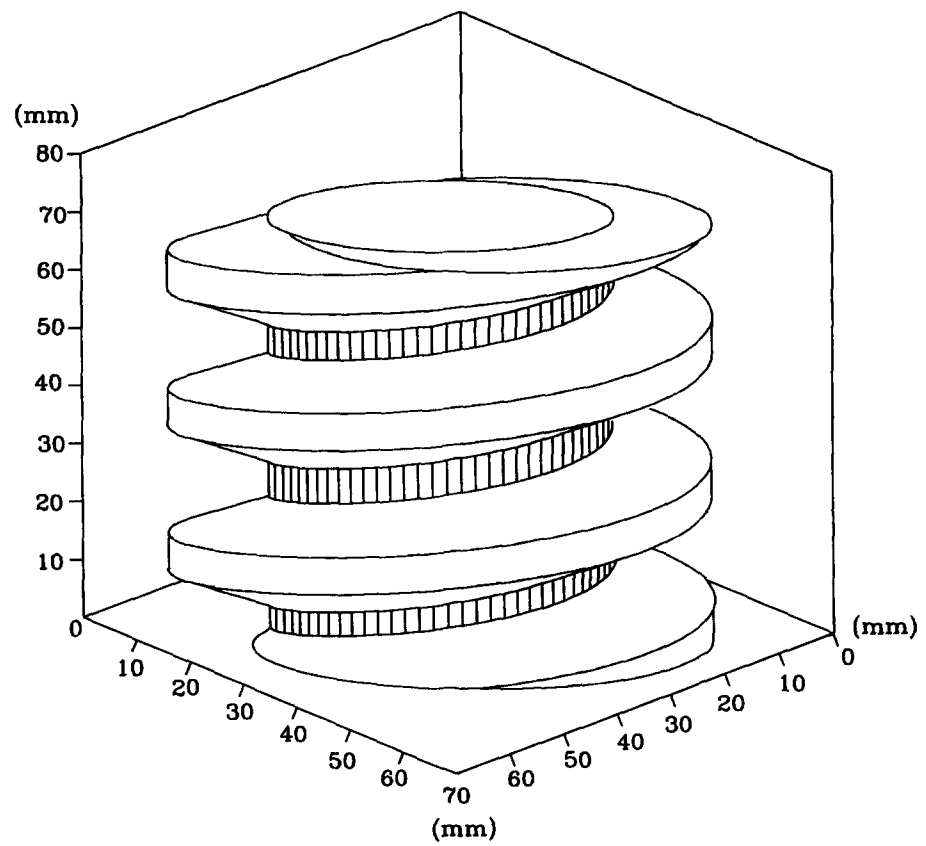

Fig. 4. Computer graphic of the worm profile.

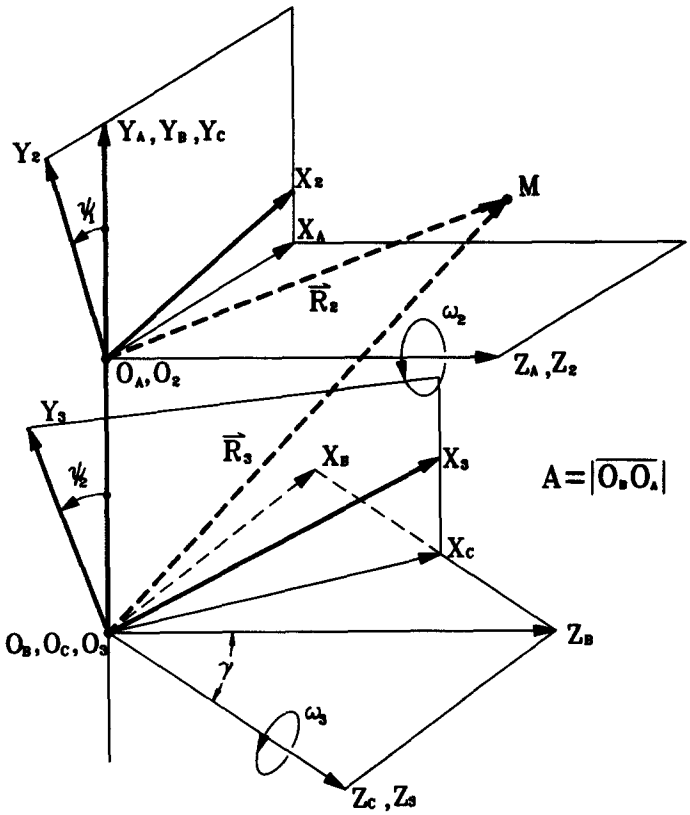

Fig. 5. Cutting mechanism of the worm and worm-gear.

convenience, the worm surface equations [i.e. equations (7) and (8)] can be represented in the reference coordinate system S_A by applying the homogeneous coordinates transformation matrix equation as follows:

$$\mathbf{R}_A = [M_{A2}]\mathbf{R}_2 \tag{10}$$

where

$$[M_{A2}] = \begin{bmatrix} \cos\psi_1 & -\sin\psi_1 & 0 & 0 \\ \sin\psi_1 & \cos\psi_1 & 0 & 0 \\ 0 & 0 & 1 & 0 \\ 0 & 0 & 0 & 1 \end{bmatrix}.$$

By substituting equations (7) and (8) into equation (10), the worm surface equation represented in coordinate system S_A becomes:

(1) The left-side worm surface

$$x_A^l = -(u\cos\alpha + r_g)\cos(\psi + \psi_1) - r_b\sin(\psi + \psi_1),$$

$$y_A^l = -(u\cos\alpha + r_g)\sin(\psi + \psi_1) + r_b\cos(\psi + \psi_1),$$

and

$$z_A^l = u\sin\alpha + p\psi + S_0. \tag{11}$$

(2) The right-side worm surface

$$x_A^r = -(u\cos\alpha + r_g)\cos(\psi + \psi_1) + r_b\sin(\psi + \psi_1),$$

$$y_A^r = -(u\cos\alpha + r_g)\sin(\psi + \psi_1) - r_b\cos(\psi + \psi_1),$$

and

$$z_A^r = -u \sin\alpha + p\psi - S_0. \tag{12}$$

NATURE OF THE CONJUGATE ACTION

Due to the conjugate action of the worm gear set, the worm and worm-gear are in continuous tangency at every moment during their meshing process. Therefore, the relative velocity of the common contact point (or line) of the worm gear set must lie on the common tangent plane. Since the tooth surface common normal vector **N** is perpendicular to the common tangent plane, the relative velocity $\mathbf{V}^{(12)}$ is perpendicular to the common normal vector **N** at the contact point or line. Therefore, the following equation must be observed

$$\mathbf{N} \cdot \mathbf{V}^{(12)} = 0. \tag{13}$$

The above equation is known in the theory of gearing as the equation of meshing for conjugate kinematic pairs. The equation of meshing relates the surface coordinates and motion parameters of conjugate kinematic pairs. In this paper, worm-gears are generated by a worm-type hob cutter. The mathematical model of the worm-gear is obtained by simultaneously considering the equation of meshing of the worm-type hob cutter and worm-gear, and the locus of the worm-type hob cutter which is represented in the worm-gear coordinate system S_3.

THE NORMAL VECTOR OF THE WORM SURFACE

If there is a surface position vector $\mathbf{R}(u, \psi) \in C^2$, where u and ψ are the surface parameters, then the normal vector **N** of this regular surface can be obtained by the equation

$$\mathbf{N} = \frac{\partial \mathbf{R}}{\partial u} \times \frac{\partial \mathbf{R}}{\partial \psi}. \tag{14}$$

Therefore, for the left-side worm surface vector $\mathbf{R}_A^l$ represented in equation (11), we have

$$\frac{\partial \mathbf{R}_A^l}{\partial u} = [-\cos\alpha \cos(\psi + \psi_1)]\mathbf{i}_A + [-\cos\alpha \sin(\psi + \psi_1)]\mathbf{j}_A + [\sin\alpha]\mathbf{k}_A$$

and

$$\frac{\partial \mathbf{R}_A^l}{\partial \psi} = [(u\cos\alpha + r_g)\sin(\psi + \psi_1) - r_b \cos(\psi + \psi_1)]\mathbf{i}_A$$
$$- [(u\cos\alpha + r_g)\cos(\psi + \psi_1) + r_b \sin(\psi + \psi_1)]\mathbf{j}_A + p\mathbf{k}_A. \tag{15}$$

By substituting equation (15) into equation (14), it is found that the normal vector of the left-side worm surface is

$$\begin{aligned}\mathbf{N}_A^l = {} & [(-p\cos\alpha + r_b \sin\alpha)\sin(\psi + \psi_1) + (u\cos\alpha + r_g)\sin\alpha\cos(\psi + \psi_1)]\mathbf{i}_A \\ & + [(p\cos\alpha - r_b \sin\alpha)\cos(\psi + \psi_1) + (u\cos\alpha + r_g)\sin\alpha\sin(\psi + \psi_1)]\mathbf{j}_A \\ & + [(u\cos\alpha + r_g)\cos\alpha]\mathbf{k}_A,\end{aligned} \tag{16}$$

where $\mathbf{i}_A$, $\mathbf{j}_A$ and $\mathbf{k}_A$ are the unit vectors of three orthogonal axes of coordinate system S_A. Similarly, according to equations (12) and (14) the normal vector of the right-side worm surface can be obtained as follows:

$$\begin{aligned}\mathbf{N}_A^r = {} & [(-p\cos\alpha + r_b \sin\alpha)\sin(\psi + \psi_1) - (u\cos\alpha + r_g)\sin\alpha\cos(\psi + \psi_1)]\mathbf{i}_A \\ & + [(p\cos\alpha - r_b \sin\alpha)\cos(\psi + \psi_1) + (u\cos\alpha + r_g)\sin\alpha\sin(\psi + \psi_1)]\mathbf{j}_A \\ & + [(u\cos\alpha + r_g)\cos\alpha]\mathbf{k}_A.\end{aligned} \tag{17}$$

RELATIVE VELOCITY AND EQUATION OF MESHING

To determine the relative velocity $\mathbf{V}^{(12)}$ between the worm and worm-gear, we must consider the meshing action of the worm and worm-gear as shown in Fig. 5. Symbols ω_1 and ω_2 are the angular velocities of the worm and worm-gear, respectively. The position vectors of any common contact

point M (X, Y, Z) represented in coordinate systems S_A and S_C are denoted by $\mathbf{R}_2$ and $\mathbf{R}_3$, respectively. The velocity at the common contact point of the worm surface, represented in coordinate system S_A, is denoted by $\mathbf{V}_A^{(1)}$. The velocity at the common contact point of the worm-gear surface, represented in coordinate system S_A, is denoted by $\mathbf{V}_A^{(2)}$. According to the meshing mechanism shown in Fig. 5, it is found that

$$\mathbf{V}_A^{(1)} = \boldsymbol{\omega}_2 \times \mathbf{R}_2 \tag{18}$$

and

$$\mathbf{V}_A^{(2)} = \boldsymbol{\omega}_3 \times \mathbf{R}_3 = \boldsymbol{\omega}_3 \times (\mathbf{O}_B\mathbf{O}_A + \mathbf{R}_2). \tag{19}$$

Therefore, the relative velocity of the worm and worm-gear is

$$\mathbf{V}_A^{(12)} = \mathbf{V}_A^{(1)} - \mathbf{V}_A^{(2)} = (\boldsymbol{\omega}_2 - \boldsymbol{\omega}_3) \times \mathbf{R}_A - \mathbf{O}_A\mathbf{O}_B \times \boldsymbol{\omega}_3. \tag{20}$$

According to Fig. 5, the angular velocities of worm and worm-gear are

$$\boldsymbol{\omega}_2 = \omega_2 \mathbf{k}_A$$

and

$$\boldsymbol{\omega}_3 = (-\omega_3 \sin\gamma)\mathbf{i}_A + (\omega_3 \cos\gamma)\mathbf{k}_A. \tag{21}$$

By substituting equation (21) into equation (20), the relative velocity becomes

$$\mathbf{V}_A^{(12)} = (A\omega_3 \cos\gamma - \omega_2 y_A + \omega_3 y_A \cos\gamma)\mathbf{i}_A + (-\omega_3 z_A \sin\gamma + \omega_2 x_A - \omega_3 x_A \cos\gamma)\mathbf{j}_A + (\omega_3 y_A \sin\gamma + A\omega_3 \sin\gamma)\mathbf{k}_A \tag{22}$$

where $A = |\overline{O_A O_B}|$. In equation (22), parameters x_A, y_A and z_A are the coordinates of worm surfaces represented in equations (11) and (12).

Since the normal vector $\mathbf{N}_A$ of the worm surface and the relative velocity $\mathbf{V}_A^{(12)}$ of the worm and worm-gear have been obtained, the equation of meshing can be determined by substituting equations (16), (17) and (22) into equation (13).

To avoid complicated expression in the derivation process, the normal vector is expressed by three components as follows:

$$\mathbf{N}_A = \begin{bmatrix} N_{Ax} \\ N_{Ay} \\ N_{Az} \end{bmatrix}. \tag{23}$$

By substituting equations (22) and (23) into equation (13), the equation of meshing is obtained as follows:

$$A\omega_3(N_{Ax}\cos\gamma + N_{Az}\sin\gamma + (\omega_2 - \omega_3\cos\gamma)(x_A N_{Ay} - y_A N_{Ax}) + \omega_3 \sin\gamma(y_A N_{Az} - z_A N_{Ay}) = 0. \tag{24}$$

With consideration of the relation $x_A N_{Ay} - y_A N_{Ax} = -pN_{Az}$ for the meshing of both sides of the worm and worm-gear surfaces, equation (24) can be simplified as follows:

$$N_{Ax}(A\omega_3 \cos\gamma) + N_{Ay}(-\omega_3 z_A \sin\gamma) + N_{Az}(A\omega_3 \sin\gamma - \omega_2 p + \omega_3 p \cos\gamma + \omega_3 y_A \sin\gamma) = 0. \tag{25}$$

Actually, equation (25) is the equation of meshing of the worm-type hob cutter and worm-gear. It relates the surface parameters u and ψ of the worm-type hot cutter, and the rotation parameters ω_2 and ω_3 of the worm-type hob cutter and the worm-gear. The worm surface coordinates x_A, y_A and z_A expressed in equation (25) are represented in coordinate system S_A, as shown in equations (11) and (12). The normal vectors of the worm surface N_{Ax}, N_{Ay} and N_{Az} are also represented in the coordinate system S_A as expressed in equations (16) and (17).

LOCUS OF THE WORM-TYPE HOB CUTTER

Since the worm-gear surface is cut with a worm-type hob cutter, the worm-gear surface equation can be obtained by finding the locus envelope of the worm-type hob cutter, represented in the worm-gear coordinate system. According to the cutting relationships shown in Fig. 5, the locus

of the worm-type hob cutter represented in coordinate system S_3 can be obtained by applying the following coordinates transformation matrix equation:

$$\mathbf{R}_3 = \begin{bmatrix} x_3 \\ y_3 \\ z_3 \end{bmatrix} = [M_{3C}][M_{CB}][M_{BA}]\mathbf{R}_A \tag{26}$$

where

$$[M_{BA}] = \begin{bmatrix} 1 & 0 & 0 & 0 \\ 0 & 1 & 0 & A \\ 0 & 0 & 1 & 0 \\ 0 & 0 & 0 & 0 \end{bmatrix} \quad [M_{CB}] = \begin{bmatrix} \cos\gamma & 0 & \sin\gamma & 0 \\ 0 & 1 & 0 & 0 \\ -\sin\gamma & 0 & \cos\gamma & 0 \\ 0 & 0 & 0 & 1 \end{bmatrix}$$

and

$$[M_{3C}] = \begin{bmatrix} \cos\psi_2 & \sin\psi_2 & 0 & 0 \\ -\sin\psi_2 & \cos\psi_2 & 0 & 0 \\ 0 & 0 & 1 & 0 \\ 0 & 0 & 0 & 1 \end{bmatrix}.$$

Parameters ψ_1 and ψ_2 are the rotation angles of the worm-type hob cutter and worm-gear, respectively, γ is the crossed angle of two rotation axes of the worm-type hob cutter and worm-gear, and A is the shortest distance between two rotation axes. By substituting equation (11) into equation (26), the locus equation of the left-side worm-type hob cutter surface, represented in coordinate system S_3, can be obtained as follows:

$$\begin{aligned} x_3 &= (p\psi + S_0 + u\sin\alpha)\sin\gamma\cos\psi_2 - [(u\cos\alpha + r_g)\sin\psi_2 + r_b\cos\gamma\cos\psi_2]\sin(\psi + \psi_1) \\ &\quad + A\sin\psi_2 - [(u\cos\alpha + r_g)\cos\psi_2\cos\gamma - r_b\sin\psi_2]\cos(\psi + \psi_1), \\ y_3 &= (-p\psi - S_0 - u\sin\alpha)\sin\gamma\sin\psi_2 - [(u\cos\alpha - r_g)\cos\psi_2 - r_b\cos\gamma\sin\psi_2]\sin(\psi + \psi_1) \\ &\quad + A\cos\psi_2 + [(u\cos\alpha + r_g)\sin\psi_2\cos\gamma + r_b\cos\psi_2]\cos(\psi + \psi_1), \end{aligned}$$

and

$$z_3 = [(u\cos\alpha + r_g)\cos(\psi + \psi_1) + r_b\sin(\psi + \psi_1)]\sin\gamma + (u\sin\alpha + p\psi + S_0)\cos\gamma. \tag{27}$$

Similarly, by substituting equation (12) into equation (26), the locus equation of the right-side worm-type hob cutter can also be obtained as follows:

$$\begin{aligned} x_3 &= (p\psi - S_0 - u\sin\alpha)\sin\gamma\cos\psi_2 - [(u\cos\alpha + r_g)\sin\psi_2 - r_b\cos\gamma\cos\psi_2]\sin(\psi + \psi_1) \\ &\quad + A\sin\psi_2 - [(u\cos\alpha + r_g)\cos\psi_2\cos\gamma + r_b\sin\psi_2]\cos(\psi + \psi_1), \\ y_3 &= (-p\psi + S_0 + u\sin\alpha)\sin\gamma\sin\psi_2 - [(u\cos\alpha + r_g)\cos\psi_2 + r_b\cos\gamma\sin\psi_2]\sin(\psi + \psi_1) \\ &\quad + A\cos\psi_2 + [(u\cos\alpha + r_g)\sin\psi_2\cos\gamma - r_b\cos\psi_2]\cos(\psi + \psi_1), \end{aligned}$$

and

$$z_3 = [(u\cos\alpha + r_g)\cos(\psi + \psi_1) - r_b\sin(\psi + \psi_1)]\sin\gamma + (-u\sin\alpha + p\psi - S_0)\cos\gamma. \tag{28}$$

THE MATHEMATICAL MODEL OF THE WORM-GEAR SURFACE

The mathematical model of the worm-gear surface can be obtained by simultaneously considering the locus equation of the worm-type hob cutter and its corresponding equation of meshing. Note that the left-side worm-type hob cutter surface cuts the right-side worm-gear surface. Therefore, system equations (25) and (27) define the surface equation of the right-side worm-gear. Similarly, system equations (25) and (28) define the surface equation of the left-side worm-gear.

In this research, the IMSL computer software package was applied to solve for these non-linear system equations. If the design parameters of the worm and worm-gear are chosen the same as

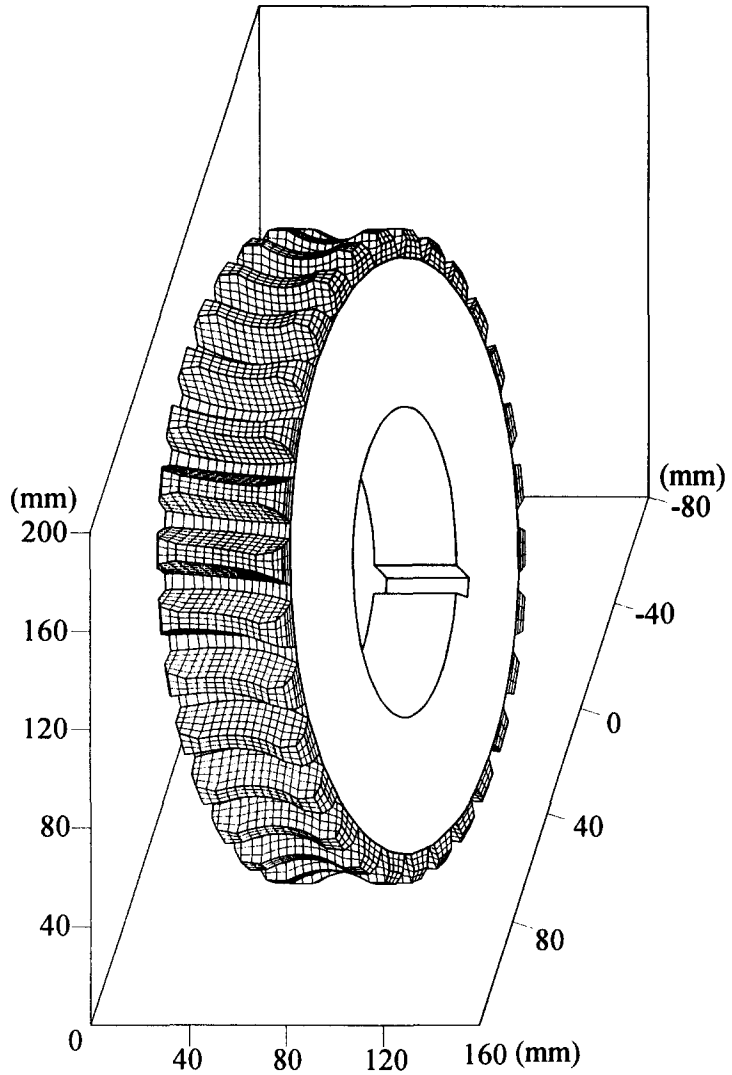

Fig. 6. Computer graphic of the worm-gear profile.

those given in previous section, then a three-dimensional computer graph of the worm-gear surfaces as shown in Fig. 6 can be obtained by applying these design data, the worm-gear surface equation and the AUTOCAD software. In addition, the cross-section of the worm gear set under meshing, as shown in Fig. 7, can also be obtained by applying the developed mathematical model of the worm gear set.

BACKLASH

In the production process, the backlash of the worm gear set should be considered to ensure smooth running. In general, an amount of ΔS_0 is added to the axial tooth thickness of the worm-type hob cutter, then the axial tooth thickness of the worm-gear is reduced by a corresponding amount of ΔS_0 to produce the backlash. However, this backlash allowance should be carefully calculated to produce minimum noise and vibration in the finished gear set. In practice, the mathematical model of the worm-type hob cutter with backlash consideration can be obtained by replacing S_0 of equations (7) and (8) by $S_0 + \Delta S_0/2$. The suggested values of the backlash for the worm gear set under various conditions can be referred to as shown by Ref. [16].

THE FLY CUTTER

For small-lot worm-gear manufacturing, gear companies always use fly cutters to manufacture worm-gears in order to reduce the product cost. The profile of the fly cutter, in fact, is the

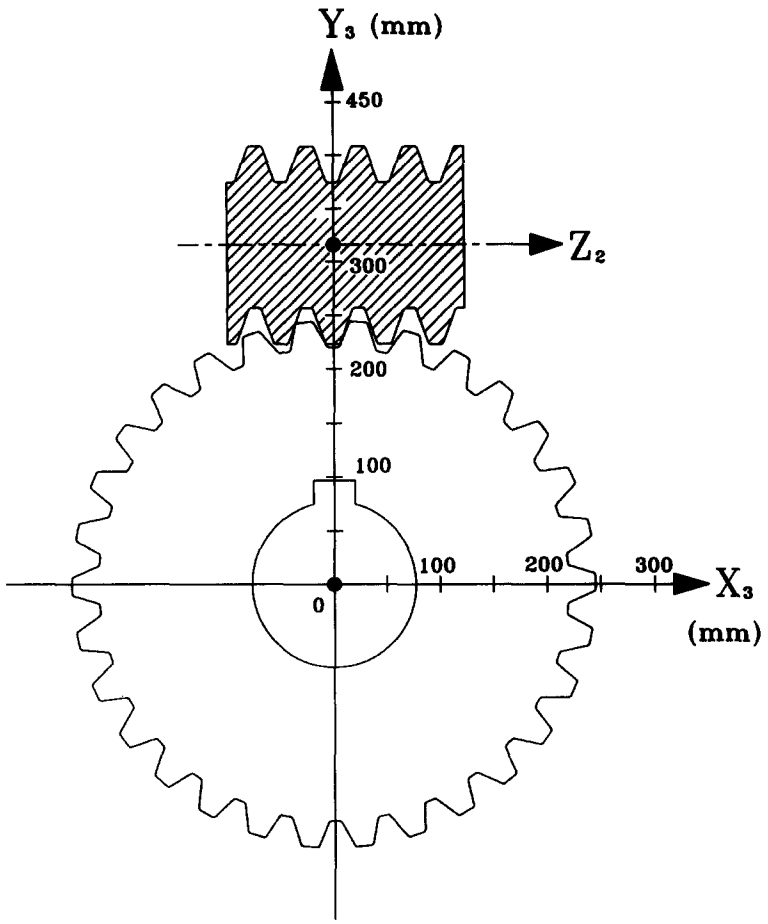

Fig. 7. Cross-section of the worm gear set under meshing.

cross-section perpendicular to the helix of the worm-type hob cutter. Figure 8 shows the relationship between the worm-type hob cutter and its normal plane to the helix. They can be related by the following equation:

$$-\tan \gamma_0 = \frac{y_2}{z_2} \tag{29}$$

where γ_0 is the lead angle of the worm-type hob cutter. By considering equation (29) and equations (7) and (8), the profile of the working portion of the fly cutter can be obtained and shown in Fig. 9.

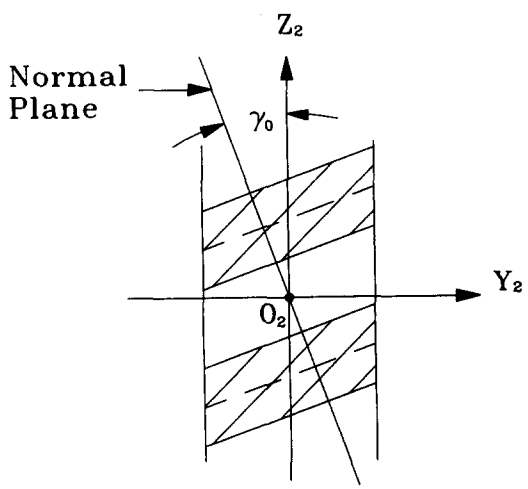

Fig. 8. Relationship between the worm-type hob cutter and its normal plane to the helix.

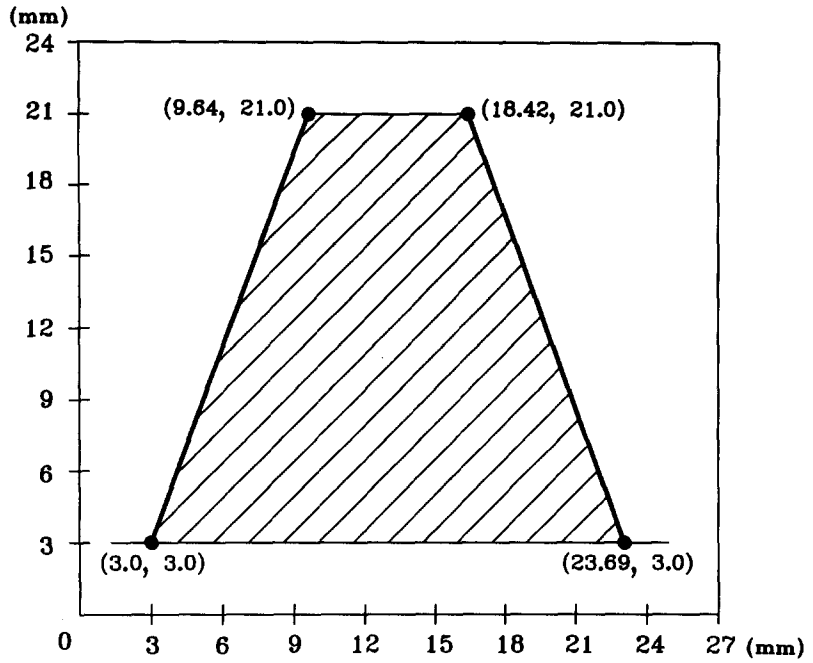

Fig. 9. Profile of the working portion of fly cutter.

CONCLUSIONS

In this paper, we have developed a mathematical model of the ZE-type worm gear set. The worm is cut by the screw motion of two cutters with straight-edged profiles, and the worm-gear surface is produced by a worm-type hob cutter. The worm equation is obtained by the locus method. Because the worm-type hob cutter and the worm-gear form a conjugate kinematic pair during the cutting process, the equation of meshing and the locus equation of the worm-type hob cutter define the mathematical model of the worm-gear. The profile of the fly cutter for small-lot worm-gear cutting, and worm-gear backlash are also investigated. The developed mathematical model is most helpful in designing, analyzing, manufacturing, measuring and optimizing worm gear set. Based on the proposed mathematical model of the worm gear set, the precise coordinates of any point on the tooth surfaces of the ZE-type worm gear set can be calculated. The calculated precise coordinates of the worm and worm-gear tooth surfaces can be used to measure the product. In addition, the developed mathematical model enables us to simulate tooth contact analysis, and can also be applied to FEM stress analysis, as well as kinematic error analysis and TCA optimization of the worm gear set.

Acknowledgement—The authors are grateful to the National Science Council of the R.O.C. for their grant. Part of this work was performed under the contract No. NSC-82-0422-E009-146.

REFERENCES

1. M. Bosch, *Klingelnberg Publication*, 3 (1988).
2. V. Simon, *J. Mech. Design* **104,** 731 (1982).
3. T. Oiwa, K. Kobayashi and A. Toyama *Prec. Engr* **12,** 85 (1990).
4. F. L. Litvin, *Gear Geometry and Applied Theory*, p. 642. Prentice Hall, New Jersey (1994).
5. H. Winter and H. Wilkesmann *J. Mech. Design* **103,** 73 (1981).
6. C. Zheng, J. Lei and M. Savage, *ASME J. Mech. Transmiss. Automn Des.* **111,** 143 (1989).
7. C. Zheng, J. Lei and M. Savage, *ASME J. Mech. Transmiss. Automn Des.* **111,** 148 (1989).
8. W. L. Janninck *et al.*, *Gear Technology* **March/April,** 31 (1988).
9. F. L. Litvin, V. Kin and Y. Zhang, *ASME J. Mech. Design* **112,** 230 (1990).
10. V. Kin, *Gear Technology* **November/December,** 30 (1990).
11. Y. C. Tsai *et al.*, *J. Chinese Soc. Mech. Engr* **2,** 135 (1990).
12. G. Bär, *Comp. Graph.* **14,** 405 (1990).
13. Cheng Shi-Chih and Liou Faa-Chyuan, *Measurement of Worm and Worm Gear*, p. 182. Bejing, China (1991).
14. F. L. Litvin and V. Kin, *ASME J. Mech. Design* **114,** 313 (1992).
15. V. Simon, *ASME Int. Power Transmiss Gearing Conf.* **1,** 73 (1992).
16. D. W. Dudley, *Handbook of Practical Gear Design*, p. 3.69. McGraw-Hill, New York (1984).